Evidence That Downregulation of Hexose Transport Limits Intracellular Glucose in 3T3-L1 Fibroblasts

RICHARD R. WHITESELL, DAVID M. REGEN, DIANA PELLETIER, AND NADA A. ABUMRAD

Measurements of initial glucose entry rate and intracellular glucose concentration in cultured cells are difficult because of rapid transport relative to intracellular volume and a substantial extracellular space from which glucose cannot be completely removed by quick exchanges of medium. In 3T3-L1 cells, we obtained good estimates of initial entry of [^{14}C]methylglucose and D-[^{14}C]glucose with *1*) L-[^{3}H]glucose as an extracellular marker together with the [^{14}C]glucose or [^{14}C]methylglucose in the substrate mixture, *2*) sampling times as short as 2 s, *3*) ice-cold phloretin-containing medium to stop uptake and rinse away the extracellular label, and *4*) nonlinear regression of time courses. Methylglucose equilibrated in two phases—the first with a half-time of 1.7 s and the second with a half-time of 23 s; it eventually equilibrated in an intracellular space of 8 μl/mg protein. Entry of glucose remained almost linear for 10 s, making its transport kinetics easier to study (K_m = 5.7 mM, V_{max} = 590 nmol · s^{-1} · ml^{-1} cell water). Steady-state intracellular glucose concentration was 75–90% of extracellular glucose concentration. Cells grown in a high-glucose medium (24 mM) exhibited a 67% reduction of glucose-transport activity and a 50% reduction of steady-state ratio of intracellular glucose to extracellular glucose. *Diabetes* 39:1228–34, 1990

Transport by facilitated diffusion is the primary route of glucose entry into cells and an important potential site for regulation of glucose metabolism. Many studies have examined the regulation of transport in cultured cells. 3T3-L1 fibroblasts have been used to investigate the acute regulation of glucose transport by insulin and its mimickers (1). Other cell types have been studied for the semiacute effect of glucose and other fuels to downregulate glucose transport (2). Glucose analogues rather than the natural substrate were used to estimate relative transport activity. Considerable differences of specificity among glucose analogues and glucose have been described in 3T3 cells (3) and L6 rat myoblasts (4). The transport behavior of a cultured cell line toward its natural hexose substrate is not accurately known, and the relationship between glucose transport and metabolism remains uncertain.

In this study, we developed a methodology for estimating initial rates of glucose and methylglucose uptake by 3T3-L1 fibroblasts. Our aim was to characterize the transport of glucose (the native substrate) and the relationship between glucose transport and metabolism in this cell line. We investigated the degree and significance of downregulation by glucose plethora.

RESEARCH DESIGN AND METHODS

3T3-L1 fibroblasts in 35-mm culture dishes were maintained with either normal low glucose (1 g/L) or high glucose (4.5 g/L) in Dulbecco's modified Eagle's medium (Difco, Detroit, MI; 5) supplemented with 10% fetal calf serum and 1% antibiotic-antimycotic solution (Sigma, St. Louis, MO) containing 10,000 U penicillin, 10 mg streptomycin, and 25 μg amphotericin B/ml in 0.9% NaCl. When almost confluent, undifferentiated cells were either used in a transport assay or detached and dispensed for reseeding. The detaching solution contained 0.05% trypsin, 0.53 mM EDTA, 0.4 g/L KCl, 0.06 g/L KH_2PO_4, 8 g/L NaCl, 0.35 g/L $NaHCO_3$, 0.09 g/L $Na_2HPO_4 \cdot 7H_2O$, 1 g/L D-glucose, and 0.01 g/L phenol red. At near confluence, each dish had ~0.5 mg cell protein measured with a protein assay kit (Bio-Rad, Richmond, CA).

HEPES-buffered salt solution (medium A) was prepared with distilled deionized water. It contained 128 mM NaCl, 10 mM HEPES, 1.4 mM $MgSO_4$, 5.2 mM KCl, 1.03 mM NaH_2PO_4, and 1.4 mM $CaCl_2$ and was adjusted to pH 7.4 with NaOH. For incubation, medium A was supplemented with 0.5% bovine serum albumin and 0.1 mM glucose (medium B).

From the Department of Molecular Physiology and Biophysics, Vanderbilt University School of Medicine, Nashville, Tennessee.

Address correspondence and reprint requests to R. Whitesell, Department of Molecular Physiology and Biophysics, Vanderbilt University School of Medicine, Nashville, TN 37232.

Received for publication 10 August 1989 and accepted in revised form 13 June 1990.

Isotopic hexose solutions were prepared as follows: ethanolic solutions of L-[^{3}H]glucose, D-[^{14}C]glucose, and [^{14}C]methylglucose (Du Pont-NEN, Boston, MA) were dried under N_2 at room temperature, dissolved in water, and deionized by passage through a 1 × 1-cm column containing DEAE-Sephadex acetate (Pharmacia, Piscataway, NJ). These solutions were made isotonic by adding 0.11 vol of 9% NaCl. The final isotopic solution was diluted fivefold with medium B and contained 2 μCi/ml L-[^{3}H]glucose and 0.5 μCi/ml D-[^{14}C]glucose or [^{14}C]methylglucose. Glucose was added from 1 M and 30 mM solutions for the transport assay.

All manipulations of cells before fixation were carried out in an Isolette infant incubator at 37°C. Before the transport assay, the growth medium was removed by aspiration, and the dish was rinsed twice with 1 ml medium B. A last aliquot of 1 ml medium B was added for a 30-min incubation. Then the medium was aspirated, and the dish was placed on a rotating shaker platform at 10 cps to start the transport assay. Isotopic hexose solution (600 μl) was pipetted onto the surface of the dish. The reaction was stopped by pipetting 2 ml chilled stop solution (medium A containing 200 μM phloretin added with stirring from a 100-mM ethanolic solution). For sampling times of <10 s, the additions of isotope and stop solution were accomplished by holding pipettes in either hand over the dish on the shaker and timing the additions by metronome. The stop solution was aspirated immediately, and the dish was quickly rinsed two more times with 2 ml stop solution. Immediately after rinsing, 1 ml 0.1 M NaOH was added to fix and extract the cells. The contents of the dish were suspended with a pipette, and 700 μl was transferred to a 20-ml scintillation vial. Five milliliters of aqueous scintillation fluid were added to this, and all samples (including counting standards and a 10-μl sample of the isotope solution) were counted under identical conditions in a three-channel counter set for double-label counting.

Uptake of [^{14}C]glucose or [^{14}C]methylglucose was expressed as normalized specific sugar space, calculated as follows: raw [^{14}C]glucose or [^{14}C]methylglucose space (μl/dish) equals total ^{14}C on the dish after rinsing (counts per minute [cpm]/dish) divided by concentration of ^{14}C in the medium (cpm/μl). Raw L-[^{3}H]glucose space was calculated as total ^{3}H on the dish after rinsing (cpm/dish) divided by ^{3}H in the medium (cpm/μl). Raw L-[^{3}H]glucose space was then subtracted from raw [^{14}C]glucose or [^{14}C]methylglucose space to yield nonnormalized specific space (μl/dish). This was routinely normalized to glucose-accessible intracellular water per dish, measured as specific [^{14}C]methylglucose space (μl/dish) after 1 h of incubation. Specific [^{14}C]glucose space normalized this way is the cell to medium concentration ratio. Glucose-accessible intracellular water is termed *cell water*. Figure 1 illustrates these calculations. Methylglucose space was normalized to cell protein to show the relationship between cell water and cell protein. Figure 1 reveals several significant technical points: L-glucose did not enter the cells at a significant rate. Raw D-glucose or methylglucose space rose from a *y*-intercept that was comparable to L-glucose space. Much of the roughness in the time course was caused by variations in removal of the extracellular label by the three rinses with stop solution. Subtracting L-glucose space effectively removed this variable blank, so specific space rose more smoothly from zero.

The rate at which cell-water–normalized specific D-glucose space rises is specific D-glucose clearance [G_o] normalized to cell water, the volume of medium containing the D-glucose entering specifically per unit of time per volume of cell water. It is also cell-water–normalized velocity (V), $V/[G_o]$, and the fractional rate of equilibration. It is convenient to express this rate as microliters of medium cleared per second per milliliter of cell water ($\mu l \cdot s^{-1} \cdot ml^{-1}$). Multiplying clearance by glucose concentration in nanomoles per milliliter gives V in nanomoles per second per milliliter. If glucose entry were unsaturable, $V/[G_o]$ would be independent of $[G_o]$, its value being the cell-water–normalized entry coefficient. If glucose entry occurs by a simple saturable process, $V/[G_o]$ will be highest (equal to V_{max}/K_m) at low $[G_o]$ and will decline toward zero with increasing $[G_o]$, $[G_o]/V$ increasing linearly with increasing $[G_o]$ (6).

Nonlinear regression was performed on data for which the models could not be easily transformed into linear relationships. The NLIN procedure (SAS, Cary, NC) was used to fit specific D-glucose or methylglucose uptake time courses with models given in RESULTS. Models were compared and

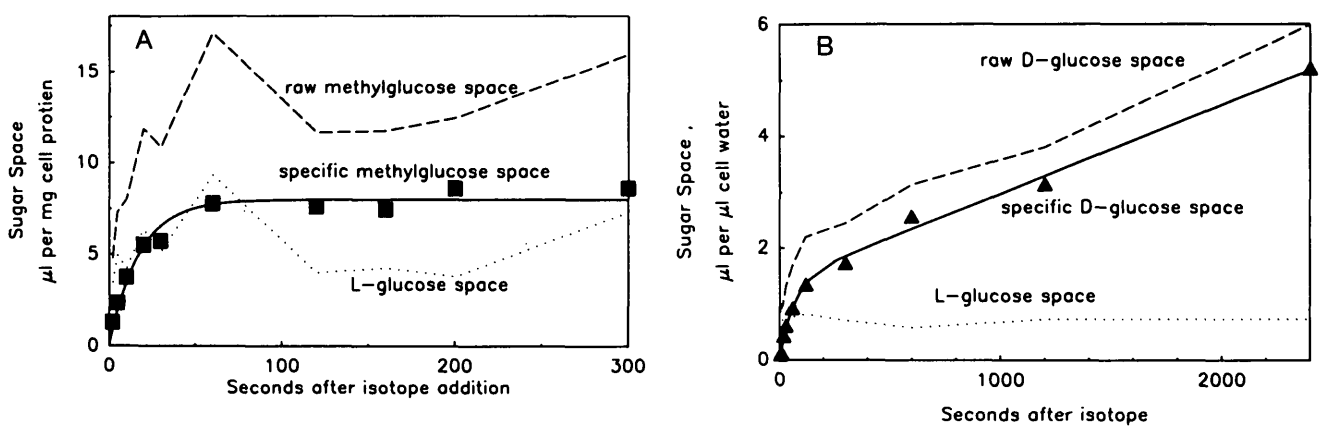

FIG. 1. Time courses of L-[^{3}H]glucose and D-[^{14}C]glucose or [^{14}C]methylglucose spaces after adding mixture of isotopes. Specific D-glucose space is raw D-glucose space minus L-glucose space. *A*: L-[^{3}H]glucose space and [^{14}C]methylglucose space expressed as microliters of medium containing amount of isotope associated with cells per milligram of cell protein. *B*: L-[^{3}H]glucose space and D-[^{14}C]glucose space expressed as microliters of medium containing amount of isotope associated with cells per microliter of cell water accessible to methylglucose.

evaluated by computing the simple correlation coefficient between observed and predicted values of the primary dependent variable (7). The correlation for the data shown and the models used was >0.95 in each case.

RESULTS

Evaluation of cell-water space. For evaluation of cell water accessible to glucose, the combination of [^{14}C]methylglucose and L-[^{3}H]glucose was used in the isotope solution (Fig. 1*A*). Cell-associated L-[^{3}H]glucose did not increase significantly after the first seconds of the time course, and this value divided by the medium L-[^{3}H]glucose concentration was taken as residual extracellular volume or space left after washing three times with stop solution. Cellular [^{14}C]-methylglucose space increased during the assay to an equilibrium value about three times the extracellular space. In four experiments, cell water estimated in this way was (mean ± SE) 7.6 ± 1.8 μl/mg cell protein.

To test for possible phosphorylation of methylglucose in this system, extracts of cells after 20 min of incubation with [^{14}C]methylglucose were passed through a 5 × 1-cm column of DEAE-Sephadex acetate and thoroughly eluted with water and then with 1 M ammonium acetate. All of the radioactivity was in the first elution, and none was in the second. Conversely, an added standard of [^{14}C]glucose-6-phosphate was completely recovered in the second elution. This indicated that there was no detectable formation of anionic metabolites, so the intracellular radioactivity represented free methylglucose.

Compartmentation of methylglucose distribution space. Time courses of methylglucose uptake with and without a high glucose concentration are shown in Fig. 2. Least-squares fitting of the uptake time course with a single-exponential model, $S_i = w(1 - e^{-\lambda t})$, revealed that this model was inadequate. The fitting curves ran under all of the data to ~50% of equilibration and then ran above all of the data in the range from 50 to 90% of equilibrium. The consistent pattern of residuals showed that methylglucose equilibrated in more than one compartment.

In contrast, the data in the composite and individual experiments were well fitted (r = 0.95) by two exponential terms

$$\text{specific methylglucose space} = w_1(1 - e^{-\lambda_1 t}) + w_2(1 - e^{-\lambda_2 t}) \quad (1)$$

With this model, the fitting curves ran among the data throughout the time course, and the residuals exhibited no consistant pattern. This and the high correlation coefficients showed that the two-compartment model was adequate and that fitting could not significantly improve by adding a third term. One compartment, w_1, comprised 35% of the cell water and equilibrated rapidly ($t_{0.5}$ = 1.7 s). Another compartment, w_2, comprised the remaining 65% and equilibrated more slowly ($t_{0.5}$ = 23 s). The initial clearance rate is given by the sum $w_1\lambda_1 + w_2\lambda_2$ = 160 ± 20 μl · s^{-1} · ml^{-1}. Data for uptake of methylglucose in the presence of 40 mM glucose were well fitted by the same model. Initial clearance was calculated as 14 ± 3 μl · s^{-1} · ml^{-1}. The 90% diminution in initial rate of methylglucose uptake caused by 40 mM glucose in the buffer is evidence that the two substrates share the same transport system (glucose-transport K_m determined in this way being ~4 mM).

The equilibrium methylglucose space was slightly but significantly reduced (~12%) when cells were incubated with 40 mM glucose. As discussed below, this indicated the presence of a modest glucose gradient across the cell membrane at steady state caused by glucose metabolism. The gradient was not large enough to indicate that transport limited glucose metabolism.

Characterization of glucose-transport kinetics. To determine glucose-transport characteristics, the combination of D-[^{14}C]glucose and L-[^{3}H]glucose was used in the isotope solution with several glucose concentrations (Fig. 3). At the lowest glucose concentration (0.1 mM), specific D-glucose space (that of glucose plus its labeled metabolites) rose >1 by ~15 s and rose to ~2.7 at 40 s, showing that a substantial fraction of cellular ^{14}C was in glucose metabolites. With each increment of glucose concentration, clearance was reduced, as expected of a saturable entry process. The reduction was 80–90% at 30–40 mM glucose, much like the effect of 40 mM glucose on methylglucose entry (Fig. 2).

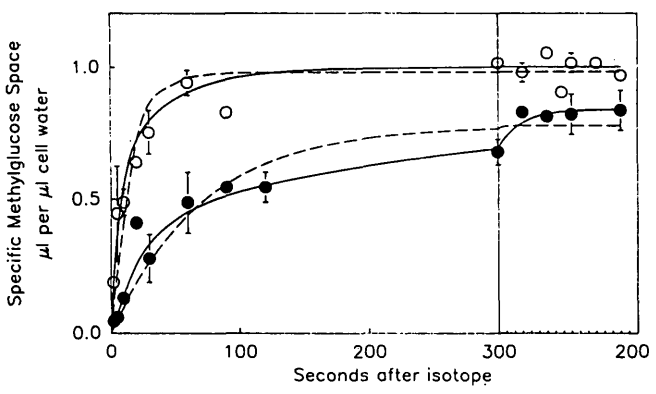

FIG. 2. Time courses of methylglucose uptake in presence of 0.1 mM (○) and 40 mM (●) medium glucose. *Bars*, SEs for points repeated in 3–5 experiments. In some cases, *bars* are smaller than *symbols*. *Dashed lines*, least-squares fitting with 1-compartment model. *Solid lines*, least-squares fitting with 2-compartment model (Eq. 1): at 0.1 mM glucose, w_1 = 350 μl/ml, λ_1 = 0.41 s^{-1}, w_2 = 650 μl/ml, and λ_2 = 0.03 s^{-1}; at 40 mM glucose, w_1 = 350 μl/ml, λ_1 = 0.04 s^{-1}, w_2 = 450 μl/ml, and λ_2 = 0.004 s^{-1}.

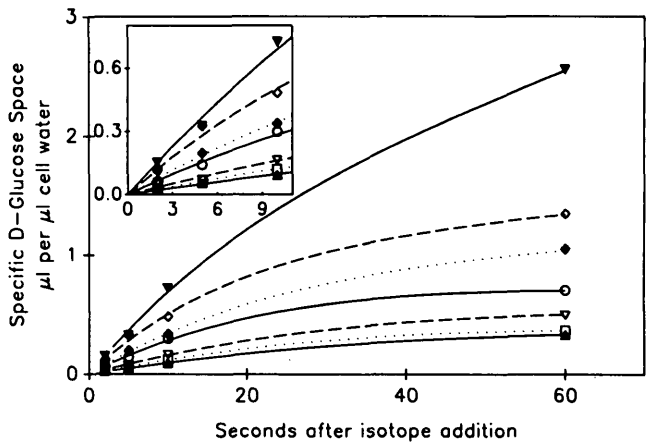

FIG. 3. Time courses of D-[^{14}C]glucose space at several glucose concentrations (in mM): ▼, 0.1; ◇, 1; ◆, 3; ○, 10; ▽, 20; □, 30; ▲, 40. Experiment typical of 3 others is shown. *Lines*, fittings with Eq. 2. *Inset*, magnification of early portion of time courses.

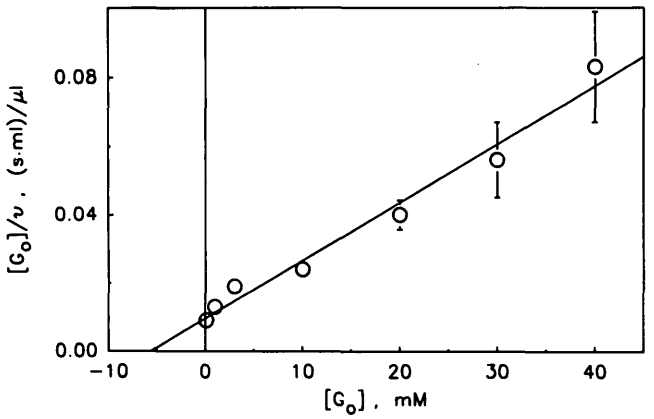

FIG. 4. Dependence of initial glucose entry on external glucose concentration displayed as Hanes plot. At lower concentrations, SEs (*bars*) are smaller than data symbols. Fit was by simple unweighted linear regression ($r > 0.97$). K_m = 5.7 mM. V_{max} = 590 nmol · s^{-1} · ml^{-1}.

The conversion of intracellular [^{14}C]glucose to [^{14}C]metabolites (which must remain in the cell until they are converted via numerous steps to CO_2, lactate, or pyruvate) tended to linearize the uptake time course (Fig. 3) compared with those of the nonmetabolized analogue methylglucose (Fig. 2). Judging from Fig. 1*B*, glucose ^{14}C label can continue accumulating in slow-turnover metabolite pools, almost linearly, for several minutes. An objective approach to estimation of initial rates is to fit the time course until 1 min with a model containing a term for the exponential approach to the steady state in a compartment and a second term for accumulation in metabolites that do not escape the cell during the 1st min

$$\text{specific D-glucose space} = w(1 - e^{-\lambda t}) + kt \qquad (2)$$

Conceptually, w is a steady-state space of glucose (and any metabolite that turns over rapidly), λ is the fractional rate of approach to the steady state, and k is the rate constant for accumulation in metabolites that do not escape during the 1st min. In practice, this is simply a model that fits [^{14}C]glucose-uptake time courses well, providing an objective estimate of initial rate supported by all of the data (8). Initial clearance is the sum $w\lambda + k$, and initial rate is initial clearance multiplied by external glucose concentration. Nonlinear regression was used to fit the time courses of Fig. 3 with this model.

Fig. 4 shows a Hanes plot of the substrate dependence. Its x-intercept is $-K_m$, and its slope is $1/V_{max}$. Linear regression indicated K_m of 5.7 ± 0.6 mM and V_{max} of 590 ± 60 nmol · s^{-1} · ml^{-1} for glucose entry.

The straight Hanes plot shows that glucose entry depends on external glucose concentration according to the simple Michaelis-Menton equation. A more complex substrate dependence (cooperativeness or entry by two mechanisms of differing saturability) results in a bent Hanes plot. Specifically, the Hanes plot would be bent concave down if glucose entered by two transporters of different K_ms, as occurs in the rat adipocyte (8), or by both saturable and unsaturable processes (9). Our data rule out significant heterogeneity of this kind in the 3T3-L1 fibroblast.

Effects of chronic exposure to high glucose concentrations. Some sets of the same cell line were grown in a high-glucose medium (4.5 g/L) and tested in parallel with cells grown in a low-glucose medium (1 g/L). Figure 5 shows the uptake of 3 mM D-[^{14}C]glucose for each group fit according to Eq. 2. The fits were good ($r < 0.95$). The initial clearances were 193 ± 12 μl · s^{-1} · ml^{-1} for low-glucose–grown cells and 64 ± 5 μl · s^{-1} · ml^{-1} for high-glucose–grown cells. Note that the growth media were rinsed away and that all cells were incubated at least 30 min in the presence of 0.1 mM glucose. Thus, the 67% reduction of transport rate by growth in a high-glucose medium represented a regulation that survived at least 30 min after the agent (glucose) was removed.

Effects of steady-state glucose gradient on equilibrium methylglucose space. Direct measurements of unlabeled intracellular glucose in cultured cells is difficult because of the small intracellular water space, the fact that steady-state glucose space would be less than the water space, and the fact that some glucose would be metabolized in the time it would take to rinse away almost all of the extracellular glucose. Direct measurements of intracellular labeled glucose would suffer from these problems and would require physical separation of glucose from its metabolites. Recognizing these problems, we chose to estimate steady-state intracellular glucose concentration from the effect of the glucose gradient on the equilibrum cell-medium methylglucose ratio, as others have done (10–12). The equilibrium cell-medium methylglucose ratio $[S_i]/[S_o]$ is proportional to the ratio of influx coefficient to efflux coefficient k_+/k_-, which is reduced <1 if there is more glucose outside competing for influx than inside competing for efflux. The relation is simple (9)

$$\text{equilibrium } \frac{[S_i]}{[S_o]} = \frac{1 + [G_i]/R_g}{1 + [G_o]/R_g} \qquad (3)$$

where R_g is the flux-ratio constant or counterflow constant of glucose. R_g is the concentration of glucose on one side of the membrane that reduces the *cis-trans* ratio of empty carrier sites by half. It is similar to the K_m of glucose entry, and we assume it to be 6 mM (9,13). The relationship can be

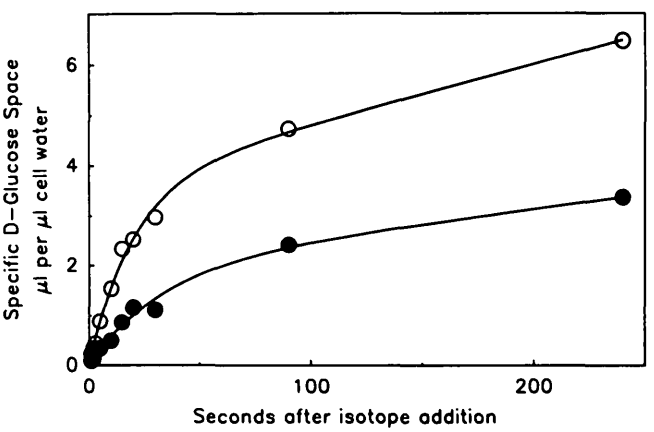

FIG. 5. Glucose-transport activity in low- and high-glucose grown cells. Cells grown for several passages in low-glucose (○) or high-glucose (●) medium was tested on same day. Glucose concentration in uptake assay was 3 mM. *Lines*, least-squares fit of data with Eq. 2.

solved for $[G_i]$ as

$$[G_i] = \left[\frac{[S_i]}{[S_o]}\left(1 + \frac{[G_o]}{R_g}\right) - 1\right] R_g \quad (4)$$

Use of this equation can be illustrated with the data from Fig. 2. With $[G_o]$ = 40 mM, R_g = 6 mM, and $[S_i]/[S_o]$ = 0.88, $[G_i]$ is computed to be 34 mM, with $[G_i]/[G_o]$ = 0.86. If the glucose concentration is relatively high, R_g need not be precisely known. For example, if R_g were assumed to be 0.1 mM, the computed $[G_i]/[G_o]$ would be 0.88; if R_g were assumed to be 15 mM, the computed $[G_i]/[G_o]$ ratio would be similar, 0.84. Because $[G_i]/[G_o]$ is not much <1, transport does not significantly limit glycolysis in these cells, which were grown in the presence of a normal glucose concentration (<5.5 mM).

We performed an experiment to estimate these quantities in basal and downregulated cells in the presence of moderate and high external glucose concentrations. Figure 6 demonstrates that methylglucose reaches an equilibrium state (where efflux is equal to influx) by 10 min in basal and downregulated cells, even in the presence of 40 mM glucose. In basal cells, 40 mM glucose reduced equilibrium $[S_i]/[S_o]$ to ~0.8, whereas in downregulated cells, 40 mM glucose reduced equilibrium $[S_i]/[S_o]$ to ~0.5. Ten millimolar external glucose reduced equilibrium $[S_i]/[S_o]$ by only 7% in basal cells but by 32% in downregulated cells (Fig. 7). These results imply much lower $[G_i]/[G_o]$ ratios in the downregulated cells, ~0.48 and 0.38 at 10 and 50 mM $[G_o]$ (Fig. 7 and Table 1). Downregulation apparently reduced $[G_i]/[G_o]$ to about half that of basal cells. At lower extracellular glucose concentrations, where glycolysis would be more substrate dependent, transport should significantly limit rates in the downregulated cells.

DISCUSSION

For more than a decade, cultured cells have become increasingly important in the study of glucose-transport regulation (1–4). Now that several different mammalian glucose transporters and enzymes of glucose metabolism have been cloned, many aspects of transport mechanism and regulation will be studied in cultured cells. Our aim was to develop and demonstrate techniques for characterizing transport of D-glucose and its nonmetabolized analogue 3-*O*-methyl-D-glucose in cultured cells.

In 3T3-L1 cells at 37°C, short sampling times were necessary for estimating initial entry rates, especially of methylglucose. This nonmetabolized sugar equilibrated in two phases, indicating two compartments, one of which had a half-time comparable to the shortest sampling time we could manage. In this case, nonlinear regression with two exponential terms was necessary for estimating initial rates. Uptake of [^{14}C]glucose was also nonlinear from our earliest sampling time, but the curvature was gentle enough that initial rates could be estimated by visualizing the first few points. Visual estimation of initial rate from a curved time course is subjective, however, and overweights the first one or two points and results in underestimation. A time-course function, with one exponential term for approach of intracellular glucose and rapid-turnover metabolites to the steady state and one linear term for accumulation in slow-turnover metabolites, fit all of the [^{14}C]glucose time courses well and allowed objective estimation of

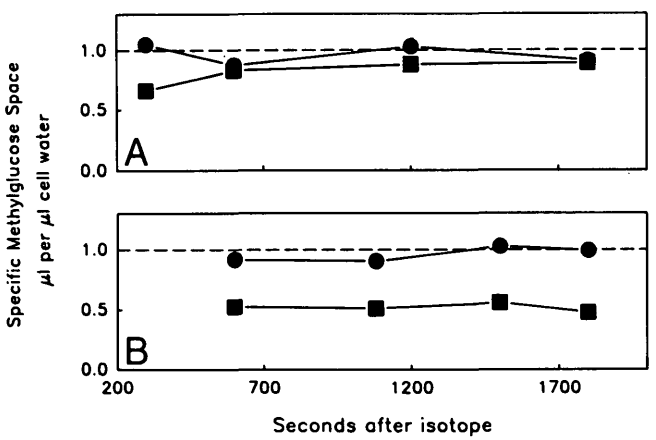

FIG. 6. Long-term uptake of tracer methylglucose in low-glucose (*A*) and high-glucose (*B*) grown cells demonstrating close approach to steady state: late points from representative time course of methylglucose uptake at 0.1 mM (●) and 40 mM (■) glucose. *Dashed line*, best fit to late methylglucose spaces obtained in presence of 0.1 mM glucose. *Solid lines* connect dishes incubated with same glucose concentration.

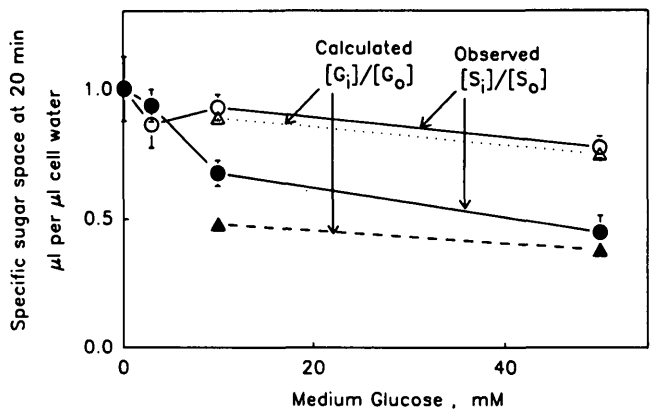

FIG. 7. Steady-state methylglucose spaces at various medium glucose concentrations in low- and high-glucose grown cells: observed methylglucose spaces ($[S_i]/[S_o]$) with 0.1, 3, 10, and 50 mM medium glucose for low-glucose–grown (○) and high-glucose–grown (●) cells tested on same day; glucose spaces ($[G_i]/[G_o]$) calculated by Eq. 4 at 10 and 50 mM medium concentration for low-glucose–grown (△) and high-glucose–grown (▲) cells.

TABLE 1
Estimation of steady-state intracellular glucose concentration

	Basal		Downregulated	
	10 mM $[G_o]$	50 mM $[G_o]$	10 mM $[G_o]$	50 mM $[G_o]$
$[S_i]/[S_o]$	0.93	0.78	0.68	0.45
$[G_i]$	8.9	37.5	4.8	19.0
$[G_i]/[G_o]$	0.89	0.75	0.48	0.38

Concentrations are millimolar. $[S_i]/[S_o]$, ratio of intracellular to extracellular methylglucose; $[G_i]$, intracellular glucose; $[G_i]/[G_o]$, ratio of intracellular to extracellular glucose.

initial entry rate, with appropriate weighting of several early points and recognition of early curvature. Because steady-state cell glucose can increase almost in proportion to medium glucose but cellular glucose-metabolite levels are limited by several factors (saturability of hexokinase, product inhibition of hexokinase, and phosphate availability), the metabolites become less significant at higher glucose concentrations.

We found that extracellular radioactivity was not completely removed by three thorough rinses of the culture dish after stopping uptake, so it was necessary to have an extracellular marker with physical properties as close as possible to those of the permeant glucose. L-[^{3}H]glucose is an ideal extracellular marker for D-[^{14}C]glucose and appears adequate for [^{14}C]methylglucose. The extracellular marker accompanied the permeant glucose or methylglucose in the substrate mixture added to the dish to initiate uptake.

We discovered that commercial labeled sugar preparations often contain labeled contaminants that are quickly and avidly taken up by or bound to cells. This artifact was prevented by passing the sugar preparations through an anion-exchange column before making up the substrate mixture in the incubation medium.

Perhaps the most impressive feature of glucose transport in 3T3-L1 cells is its high activity in relation to cell water and glycolytic rate. In basal cells (grown in a normal medium), methylglucose equilibrates in a cellular compartment with a half-time of ~1.7 s and in another compartment with a half-time of ~23 s. [^{14}C]glucose space (incuding free glucose and metabolites) exceeds the water space within 15 s after the addition of 0.1 mM [^{14}C]glucose. At 10–50 mM extracellular glucose, the steady-state cell to medium glucose concentration ratio is ~0.75–0.9, which is only 10–25% less than what it would be if transport activity were infinite. In basal cells, therefore, there is a plethora of transport activity, and transport does not significantly limit glucose use. Under these circumstances, characterization of glucose transport must involve techniques comparable to those used here, with a reliable extracellular marker, early sampling times, and nonlinear regression of time courses. Specifically, 5–10 min deoxyglucose uptake and 10–30 min ^3H_2O production from [^{3}H]glucose would reflect glycoiytic enzyme activities rather than transport activity.

The 3T3-L1 cell exhibits marked feedback regulation of transport. Growth in 24 mM glucose resulted in a 67% reduction of glucose-transport activity. This reduced the steady-state cell to medium glucose concentration ratio to about half of that in basal cells. At low extracellular glucose concentrations, transport might limit rates significantly more in downregulated cells than in basal cells. At 10–50 mM glucose concentration, however, there remained a plethora of transport activity even after downregulation. Glycolysis would not be expected to be significantly reduced by a reduction of [G_i] from 8.9 to 4.8 mM, because these concentrations are well above the K_m of hexokinase. The K_m of glycolysis is sometimes much higher than the K_m of hexokinase, however, so we cannot exclude a significant effect of downregulation on glucose use at physiological glucose concentrations (14). At least one biological process is sensitive to glucose concentration in this range, because the downregulation itself is a response to an increase of glucose concentration above normal.

The two phases of methylglucose equilibration differed by >10-fold in equilibration half-time. We do not know whether this represents differences among cells (perhaps because of different phases of their division cycle) or intracellular organelles equilibrating slower than the cytosol. Despite this compartmental heterogeneity, there was no detectable heterogeneity of entry mechanism such as we observed in adipocytes (8). The Hanes plot of the dependence of initial glucose entry on external glucose was essentially straight, not bent concave down as would be the case if glucose entered by two or more transporters with different affinities or by saturable and unsaturable processes. The K_m was ~6 mM, comparable to that of muscle (10) and the blood-brain barrier (15) and well below that of liver (16). The kinetics were consistant with the type of glucose transporter detected in these cells by molecular biology techniques. Northern blots revealed mRNA corresponding to the brain-erythrocyte-HepG2 glucose transporter and not to the liver glucose transporter or the insulin-regulatable glucose transporter (data not shown).

In some important respects, this study differs from other studies of transport in cultured cells. First, glucose was used as a substrate for the transport studies so that its transport parameters could be directly estimated. Second, we used early sampling times to help estimate initial rates, a precaution that was vindicated by the early departure from linearity of time courses of uptake of both glucose and methylglucose. Third, we believe this to be the first demonstration of an adaptive glucose-transport modulation that resulted in the transport step becoming restrictive to availability of intracellular glucose.

ACKNOWLEDGMENTS

This work was supported by National Institutes of Health Grant DK-33301 (N.A.A.) and Juvenile Diabetes Foundation Grants 18665 and 181563 (R.R.W.).

REFERENCES

1. Frost SC, Lane MD: Evidence for the involvement of vicinal sulfhydryl groups in insulin-activated hexose transport by 3T3-L1 adipocytes. *J Biol Chem* 260:2646–52, 1985
2. Ullrey DB, Franchi A, Pouyssegur J, Kalckar HM: Down-regulation of the hexose transport system: metabolic basis studied with a fibroblast mutant lacking phosphoglucose isomerase. *Proc Natl Acad Sci USA* 79:3777–79, 1982
3. Romano AH: Transport of 6-deoxy-D-glucose and D-xylose by untransformed and SV40-transformed 3T3 cells. *J Cell Physiol* 89:737–44, 1976
4. D'Amore T, Lo TCY: Hexose transport in L6 rat myoblasts. I. Rate-limiting step, kinetic properties, and evidence for two systems. *J Cell Physiol* 127:95–105, 1986
5. Dulbecco R, Freeman G: Plaque production by the polyoma virus. *Virology* 8:396–97, 1959
6. Segel IH: *Enzyme Kinetics*. New York, Wiley, 1975
7. Afifi AA, Azen SP: *Statistical Analysis: A Computer Oriented Approach*. 2nd ed. New York, Academic, 1979
8. Whitesell RR, Regen DM, Abumrad NA: Evidence for functionally distinct glucose transporters in basal and insulin-stimulated adipocytes. *Biochemistry* 28:6937–43, 1989
9. Regen DM, Morgan HE: Studies of the glucose-transport system in the rabbit erythrocyte. *Biochim Biophys Acta* 79:151–66, 1964
10. Morgan HE, Regen DM, Park CR: Identification of a mobile carrier-mediated sugar transport system in muscle. *J Biol Chem* 239:369–74, 1964
11. Crofford OB: Countertransport of 3-*O*-methylglucose in incubated rat epididymal adipose tissue. *Am J Physiol* 212:217–20, 1967

12. Foley JE, Cushman SW, Salans LB: Intracellulcar glucose concentration in small and large rat adipose cells. *Am J Physiol* 238:E180–85, 1980
13. May JM, Mikulecky DC: Glucose utilizatioin in rat adipocytes. *J Biol Chem* 258:4771–77, 1983
14. Morgan HE, Regen DM, Henderson MJ, Sawyer TK, Park CR: Regulation of glucose uptake in muscle. VI. Effects of hypophysectomy, adrenalectomy, growth hormone, hydrocortisone, and insulin on glucose transport and phosphorylation in the perfused rat heart. *J Biol Chem* 236:2162–68, 1961
15. Buschiazzo PM, Terrell EB, Regen DM: Sugar transport across the blood-brain barrier. *Am J Physiol* 219:1505–13, 1970
16. Williams TF, Exton JH, Park CR, Regen DM: Stereospecific transport of glucose in the perfused rat liver. *Am J Physiol* 215:1200–209, 1968